Bioorganic & Medicinal Chemistry Letters 20 (2010) 7159–7163

Contents lists available at ScienceDirect

Bioorganic & Medicinal Chemistry Letters

journal homepage: www.elsevier.com/locate/bmcl

The novel benzopyran class of selective cyclooxygenase-2 inhibitors. Part 2: The second clinical candidate having a shorter and favorable human half-life

Jane L. Wang *, David Limburg, Matthew J. Graneto, John Springer, Joseph Rogier Bruce Hamper, Subo Liao, Jennifer L. Pawlitz, Ravi G. Kurumbail, Timothy Maziasz, John J. Talley, James R. Kiefer *, Jeffery Carter

Pfizer Global Research and Development, 700 Chesterfield PKWY West, Chesterfield, MO 63017, USA

ARTICLE INFO

Article history:
Revised 12 July 2010
Accepted 14 July 2010
Available online 24 July 2010

Keywords:
Cyclooxygenase
COX-2 inhibitor
Clinical candidate
Benzopyran
Half-life
Plasma protein bound
Microsomal
X-ray crystal structure

ABSTRACT

In this Letter, we provide the structure–activity relationships, optimization of design, testing criteria, and human half-life data for a series of selective COX-2 inhibitors. During the course of our structure-based drug design efforts, we discovered two distinct binding modes within the COX-2 active site for differently substituted members of this class. The challenge of a undesirably long human half-life for the first clinical candidate **1** $t_{1/2}$ = 360 h was addressed by multiple strategies, leading to the discovery of **29b**-(***S***) (SC-75416) with $t_{1/2}$ = 34 h.

In part 1 of this investigation we described substituted 2-trifluoromethyl-2*H*-benzopyran-3-carboxylic acids as a novel series of potent and selective cyclooxygenase-2 (COX-2) inhibitors. We discussed the discovery of the first clinical candidate **1** (SD-8381) (Fig. 1) which had excellent potency and efficacy as an analgesic and anti-inflammatory agent.[1a]

Despite its favorable half-life in rats ($t_{1/2}$ = 10.1 h), dogs ($t_{1/2}$ = 20.4 h), and cyno ($t_{1/2}$ = 14.2 h),[1b] its half-life in humans was strikingly higher ($t_{1/2}$ = 360 h). The route of clearance was not consistent across species. The primary clearance pathway in rat and dog was as parent (feces); whereas, in the cyno the primary clearance was as the acyl-glucuronide phase-2 metabolite (urine). In vitro human microsomal metabolism study of analog **1** (100% remaining) showed no evidence of phase-1 metabolism. We reasoned that incorporation of a new clearance pathway, common across multiple species, might provide a higher probability of identifying a compound with a more predictable human half-life. Commonly, leads having too short a half life are re-engineered by the iterative identification and blocking of metabolic sites with oxidatively stable moieties. We reasoned that incorporation of metabolically labile moieties might provide a path to shorten the half-life of **1**. We also incorporated polar groups to lower log *P* and decrease plasma protein binding as a means of shortening the in vivo half-life.

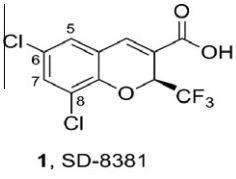

1, SD-8381

$t_{1/2}$ rat = 10.2 h, human = 360 h
hCOX-1[a] IC_{50} = 0.69 uM
hCOX-2[a] IC_{50} = 0.01 uM
Air pouch[b] ED_{50} = 0.54 mg/kg
Edema[c] ED_{50} = 7.1 mg/kg
Hyperalgesia[d] ED_{50} = 2.6 mg/kg
Adj. Arth.[e] ED_{50} = 0.03 mg/kg

Figure 1. SD-8381, a lead COX-2 inhibitor. (see Part 1 of this Letter). (a) See Ref. 2 section 2.4 and note 3. (b) See Ref. 2 section 2.9. (c) and (d) See Ref. 2a–c section 2.10. (e) See Ref. 2a–c Section 2.11.

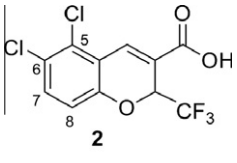

2

hCOX-1[a] IC_{50} = 0.69 uM
hCOX-2[a] IC_{50} = 0.01 uM

Figure 2. Compound **2**, an analog of COX-2 inhibitor. (see Part 1 of this Letter). (a) See Ref. 2c Section 2.4 and note 3.

* Corresponding authors. Tel.: +1 636 527 5037; fax: +1 636 247 2086 (J.L.W.); tel.: +1 636 207 1048 (J.R.K.).
E-mail addresses: jl47wang@yahoo.com (J.L. Wang), james.kiefer@att.net (J.R. Kiefer).

0960-894X/$ - see front matter © 2010 Elsevier Ltd. All rights reserved.
doi:10.1016/j.bmcl.2010.07.054

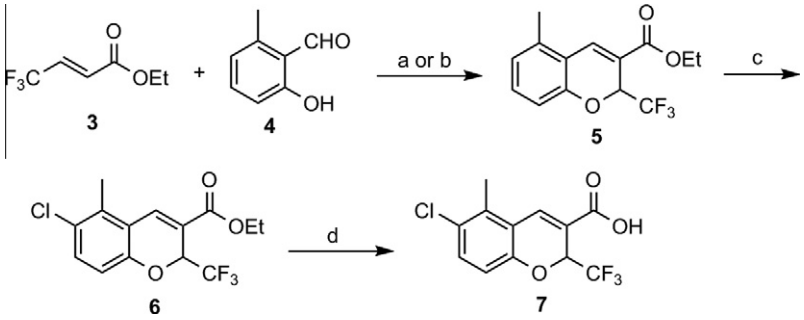

Scheme 1. Reagents and conditions: (a) K_2CO_3, DMF, 80–100 °C; (b) Et_3N, DMSO; (c) (I) HOAc, Cl_2, (II) Zn dust; (d) NaOH, THF, CH_3OH, H_2O.

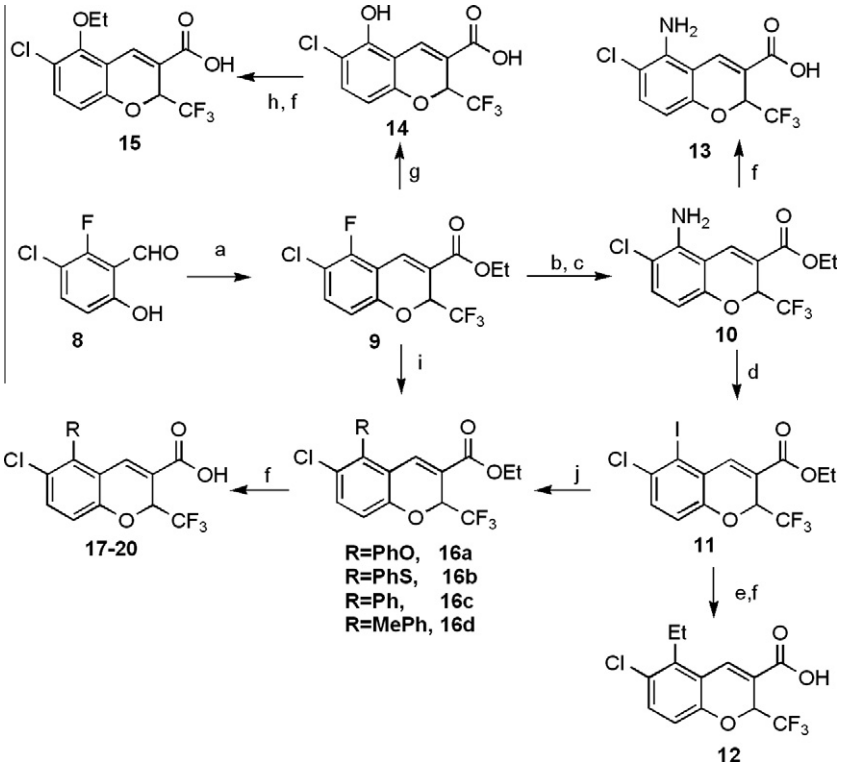

Scheme 2. Reagents and conditions: (a) **3**, K_2CO_3, DMF, 80–100 °C; (b) NaN_3, DMSO, H_2O, 85 °C, 15 h; (c) $SnCl_2$–$2H_2O$, MeOH; (d) 47% aq HI, KNO_2, DMSO, 35 °C; (e) tetrakis triphenylphosphine–palladium(0), K_2CO_3, $B(Et)_3$, DMF, 110 °C, 5 h; (f) LiOH–H_2O, THF, H_2O, EtOH, 80 °C, 4 h; (g) 2-methylsulfonylethanol, NaH, DMF, 0 °C; (h) CH_3CH_2Br, Cs_2CO_3, DMF; (i) HOPh or HSPh, K_2CO_3, DMF, 110 °C; (j) tetrakistriphenyl phosphine–palladium(0), $RB(OH)_2$, DMA, 2.0 M aq Na_2CO_3, 95 °C, 16 h.

Table 1
SAR of 5-substituted benzopyran analogs

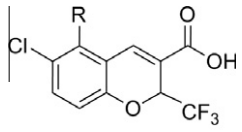

7, 12-13,15, 17-20

Compd	R	Mod human IC_{50}[a] (μM)		*c* log *P*
		COX-1	COX-2	
7	Me	7.44	0.12	4.37
12	Et	66.7	28.8	4.90
13	NH_2	>100	1.48	2.89
15	EtO	>100	>100	4.19
17	PhO	39.8	0.53	5.74
18	PhS	48.9	0.34	6.24
19	Ph	68.4	4.64	5.51
20	MePh	0.37	1.98	6.01

IC_{50} curves were generated with each test concentration run in duplicate, each curve was done $n \geqslant 2$. The high concentration was 500 μM.
[a] See Ref. 2c Section 2.4 and note 3.

Table 2
SAR of 6,8-diCl-7-alkoxy analogs **23a–e**

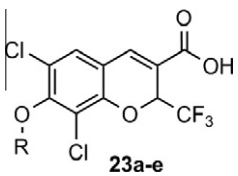

23a-e

Compd	R	Mod human IC_{50}[a] (μM)		*c* log *P*
		COX-1	COX-2	
23a	$-CH_2$c-pentyl	<0.14	<0.006	6.26
23b	$-CH_2CH(CH_2CH_3)_2$	<0.14	0.021	6.68
23c	$-C(CH_3)_3$	<0.14	0.028	5.41
23d	$-CH_2CH(CH_3)_2$	0.002	0.028	5.63
23e	$-CH_2$ *c*-hexyl	3.79	0.034	6.82

IC_{50} curves were generated with each test concentration run in duplicate, each curve was done $n \geqslant 2$. The high concentration was 500 μM.
[a] See Ref. 2c Section 2.4 and note 3.

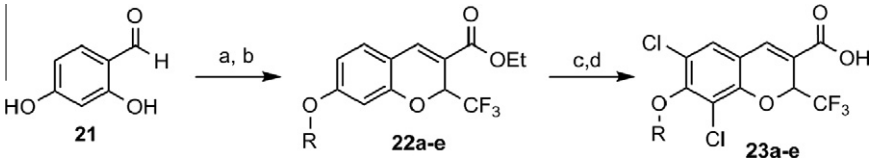

Scheme 3. Reagents and conditions: (a) **3**, DMSO, Et3 N, heat; (b) polymer–PPh_3, DEAD, THF; (c) Cl_2, HOAc; (d) NaOH, EtOH, THF, H_2O.

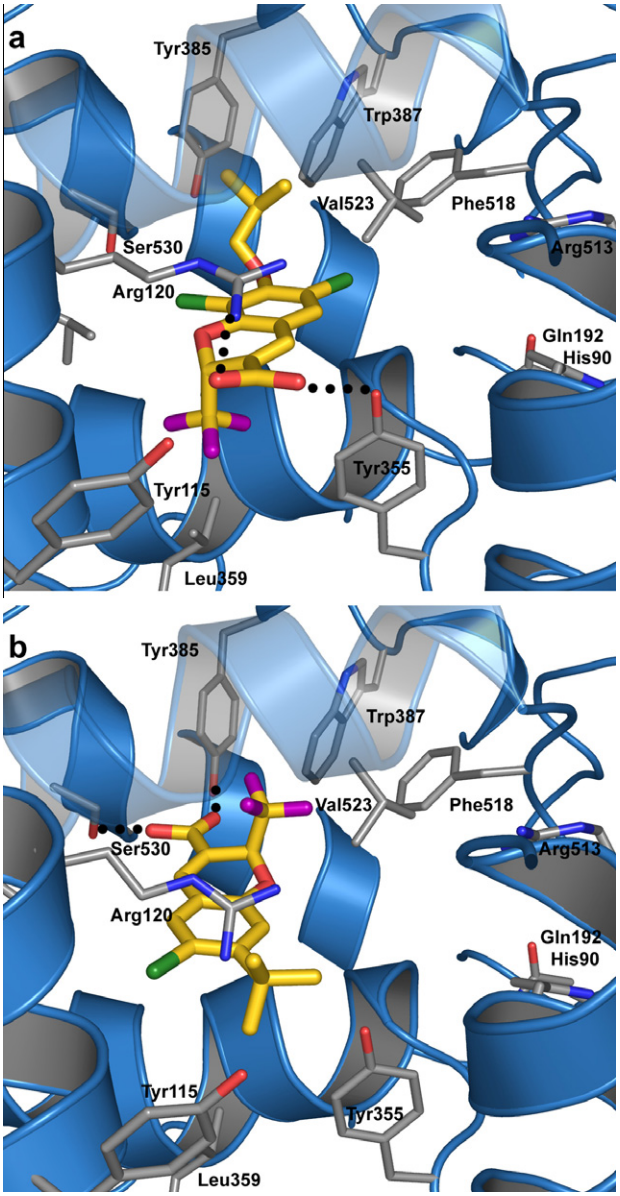

Figure 3. Crystal structures of inhibitors (a) **23d**-(***R***) and (b) **29b**-(***S***) bound at the COX-2 active site [composed with PyMol]. Note that the orientation of the compounds differs by approximately 180° and that the chirality of the stereo center inverts between the two structures.

As discussed in part 1 of this Letter, 6-substitution was required for potency. Based on the biological data of compound **2** (Fig. 2) (analog **5a** in part 1 of this Letter), we modified the 5-position of the benzopyran by introducing alkyl and aryl groups to further optimize the activity while maintaining the chloro at the 6-position (Scheme 2). The 5-Me-6-Cl acid **7** was prepared via a three step-reaction;[4] first formation of the 5-Me chromene **5**, followed by chlorination (**6**) and then hydrolysis as described in Scheme 1. 5-Amino derivative, **10**, was prepared from **8** by conversion to **9**, followed by treatment with azide followed by reduction with $SnCl_2$. 5-I chromene **11** was obtained by treating **10** with KNO_2 and HI. Palladium mediated coupling of **11** with triethylborane and hydrolysis provided **12**. 5-Amino acid **13** was obtained by hydrolysis of ester **10**. Treatment of **9** with 2-methylsulfonyl ethanol and sodium hydride produced phenol **14**. Alkylation of **14** with ethyl bromide followed by ester hydrolysis provided acid **15**. Compounds **16a** and **16b** were obtained by nucleophilic displacement of 5-F chromene **9** with phenol, thiophenol. Analogs **16c** and **16d** were prepared by Suzuki coupling of **11** with the appropriate boronic acids. The esters (**16a–d**) were hydrolyzed to afford acids **17**–**20**. Table 1 showed while the 5,6-diCl acid **2** exhibited optimal potency, all other groups at the 5-position (**7**, **12**, **13**, **15**, **17**–**20**) had greatly decreased potency of hCOX-2.

Initial SAR exploration of the 5-position did not lead to a sufficiently potent COX-2 inhibitor to warrant further consideration. Based on the desirable characteristics of **1** (SD-8381), we introduced polar moieties or metabolizable groups at the 7-position of **1** to examine their effect on activity. Compounds **23a–e** were prepared from the salicylaldehyde **21** to form the chromene ester, followed by a Mitsunobu reaction to provide 7-alkoxy esters **22a–e**, which upon chlorination and hydrolysis provided 7-alkoxy acids **23a–e** (Scheme 3). Table 2 shows that these analogs were very potent COX-2 inhibitors, but not as selective as compound **1**. We also observed a departure from the basic SAR trends previously seen in the benzopyran series when lengthy 7-substitutions were made (data not shown). To explore this divergence in SAR, we determined the crystal structure of bound (*R*,*S*) **23d** at 2.2 Å resolution (see Supplementary data for methods and data statistics). Only the (*R*-isomer) was bound in the active site. It was observed that **23d**-(***R***) had inverted and that the binding mode of the compound was rotated 180° (Fig. 3a and Note 5). This result was further confirmed by obtaining the crystal structure of the resolved **23d**-(***R***) and failing to obtain crystals with **23d**-(***S***). In this new binding mode, the *R*-isomer bound much like typical NSAIDs and had formed a 2.5 Å hydrogen bond to Tyr355 (numbering based on ovine COX-1) and a 3.0 Å ion pair with Arg120.[6] The trifluoromethyl group formed van der Waals interactions with Leu351 and Phe367, similar to celecoxib,[1a] though the connection angle to the core differs. The 7-alkoxy tail extended into the top of the active site, sweeping out approximately the same space as the trifluoromethyl group of the *S*-isomer binding orientation and of the 4-methyl aryl ring of celecoxib. In this orientation, the 5-position rather than the 8-position of the compound pointed towards the side pocket of the active site. By contrast, the 8-position, which could tolerate large substituents in the *S*-enantiomer binding mode was flanked by a hydrophobic patch of residues including Val345 and Leu531 with limited space for elaboration. Since the binding mode and stereochemical preference changed with the addition of long 7-alkoxy substitutions, an entirely new SAR pattern governs the binding of *R*-enantiomers in this sub-series. Intriguingly, COX-2 selectivity was retained in the *R*-isomer binding mode in spite of changing every protein–inhibitor interaction and the anecdotal observation that NSAIDs formed ion pairs to Arg120 tend to lack COX isoform selectivity.

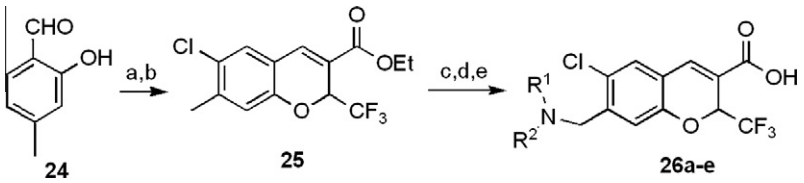

Scheme 4. Reagents and conditions: (a) K_2CO_3, Et_3N, DMF, 60–90 °C, 84% yield; (b) Cl_2 (g), AcOH, Zn dust, 80% yield; (c) NBS, $(BzO)_2$, CCl_4, reflux, 85% yield; (d) HNR^1R^2, K_2CO_3, DMF, 0 °C; (e) NaOH, THF, CH_3OH, H_2O, two steps 18–57% yield.

Table 3
Analogs with polar groups at the 7-position decreased hCOX-2 inhibition

Compd	R^1/R^2	Mod human IC_{50}[a] (μM)		*c* log *P*
		COX-1	COX-2	
26a	$-N(CH_3)(CH_2CH_3)$	100	21.3	1.96
26b	$-N(CH_3)[CH(CH_3)_2]$	100	100	2.27
26c	2,5-diMe pyrrolidine	100	96	3.11
26d	$-N[CH(CH_3)_2]_2$	100	100	3.11
26e	2,6-diMe piperidine	100	62.2	3.66

IC_{50} curves were generated with each test concentration run in duplicate, each curve was done $n \geqslant 2$. The high concentration was 500 μM.
[a] See Ref. 2c Section 2.4 and note 3.

Keeping the key 6-chloro substituent and removing the 8-chloro to reduce the *c* log *P*, we explored the 7-position extensively by both parallel and conventional chemical synthesis. First, we explored the 7-position by introduction of polar moieties such as methyl amino groups to lower the *c* log *P* ranging from 2 to 3.7. Methyl salicylaldehyde **24** was converted to the chromene and then chlorinated to form the ester **25** via similar steps described at Scheme 1. After bromination of 7-methyl **25**, we replaced the bromo with various amines, then hydrolyzed the ester to provide acids **26a–e** (Scheme 4). Unfortunately, none of these amine analogs maintained COX inhibition (Table 3).

We focused on analogs without basic moieties, but having reasonable lipophilicity and bearing the metabolizable groups to reach our goal in lowering half-life. Compounds were designed and prepared according to Scheme 5. Starting with phenol **27**, the salicylaldehyde was formed, which was then converted to the chromene ester **28**.[4] Acids **29a–e** were obtained first via 9-BBN coupling with 7-iodo chromene **28**, followed by chlorination and hydrolysis. Analogs **32a–b** were prepared by nucleophilic displacement of 7-fluoro chromene **30** with nucleophilic thiol or amine to form the 7 substituted analogs **31a–b**, followed by hydrolysis as described in Scheme 6. Alkoxy analog **33** was prepared according to Scheme 3 except less chlorine gas was used compared when preparing di-chloro analogs. The SAR in Table 4 revealed that compound **29a**, with a smaller group at the 7-position, was a less potent COX-2 inhibitor. However, analogs **29b–e**, **32a–b**, and **33**, with bulky or longer groups at the 7-position, displayed potent COX-2 inhibition.

Table 4
Analogs with metabolized groups at the 7-position displayed hCOX-2 inhibition

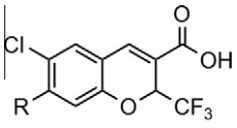

29a-e, 32a-b, 33

Compd	R	IC_{50}[a] Mod. h COX-2 (μM)	Micros. (%) rem. human/rat	Air pouch (10 mpk)[b] (%)
29a	$-CH(CH_3)_2$	0.30	n.d.	n.d.
29b	$-C(CH_3)_3$	0.005	51/n.d.	100
29c	$-CH_2CH_2CH_3$	0.15	0.71/0.26	49
29d	$-CH_2CH(CH_3)_2$	0.020	0.49/0.44	62
29e	$-(CH_2)_2C(CH_3)_2$	0.094	0.86/0.86	51
32a	$-SCH_2CH(CH_3)_2$	0.019	0.75/0.38	30
32b	$-N(CH_3)CH_2CH(CH_3)_2$	0.070	0.54/0.51	52
33	$-OCH_2CH(CH_2CH_3)_2$	0.046	0.76/0.73	42

IC_{50} curves were generated with each test concentration run in duplicate, each curve was done $n \geqslant 2$. The high concentration was 500 μM.
[a] See Ref. 2c Section 2.4 and note 3.
[b] See Refs. 2a–c Section 2.9.

We determined the 2.8 Å resolution crystal structure of the most potent enantiomer of **29b** and observed the *S*-enantiomer bound at the COX-2 active site. No co-crystals were obtained from the opposite enantiomer. The orientation of **29b**-(***S***) matches that of the previously reported *S*-isomer structure (**1**)[1a] and preserves many of the same contacts between the protein and inhibitor.

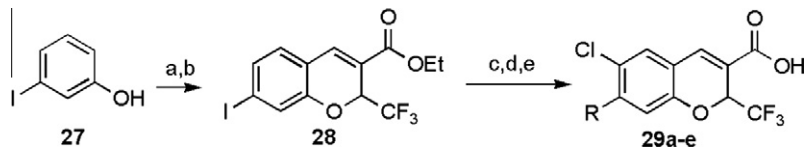

Scheme 5. Reagents and conditions: (a) $MgCl_2$, ACN, *p*-formaldehyde, TEA, 10–72 °C, 2 h, 79% yield; (b) K_2CO_3, DMF, 80–100 °C, 71% yield; (c) R-9BBN, THF, $Pd(dppf)Cl{\cdot}CH_2Cl_2$, K_3PO_4(aq), 60 °C, 4 h, 56–76% yield; (d)HOAc, Cl_2, Zn dust, 100% yield; (e) NaOH, THF, CH_3OH, H_2O, 91% yield.

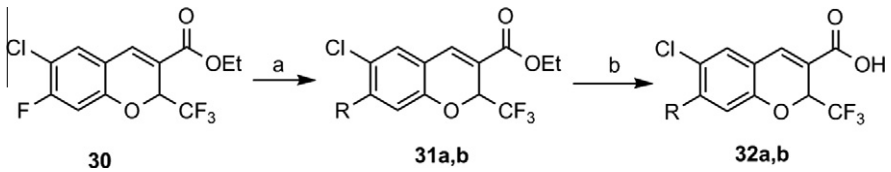

Scheme 6. Reagents: (a) HSR or HNR^1R^2, K_2CO_3, DMF, 80–100 °C, 48 h, 80–90% yield; (b) NaOH, THF, CH_3OH, H_2O, 90% yield.

Table 5
S and *R* enantiomers of 7-substituted chromenes displayed different hCOX-2 inhibition

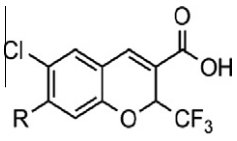

29a-e, 32a-b

Compd	R	*S*-isomer		*R*-isomer	
		Mod h COX-1	IC_{50}[a] (μM) COX-2	Mod h COX-1	IC_{50}[a] (μM) COX-2
29b	$-C(CH_3)_3$	1.02	0.062	136	5.15
29c	$-CH_2CH_2CH_3$	1.95	0.14	0.44	0.005
29d	$-CH_2CH(CH_3)_2$	100	0.91	0.35	0.007
29e	$-(CH_2)_2C(CH_3)_2$	41.6	1.13	1.63	0.068
32a	$-SCH_2CH(CH_3)_2$	22.6	0.15	3.66	0.008
32b	$-N(CH_3)CH_2CH(CH_3)_2$	100	0.87	15.8	0.085

IC_{50} curves were generated with each test concentration run in duplicate, each curve was done $n \geqslant 2$. The high concentration was 500 μM.
[a] See Ref. 2c Section 2.4 and note 3.

Table 6
Pharmacology of **29b-(*S*)** (SC-75416)

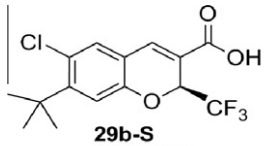

$t_{1/2}$ (rat) = 4 hr
$t_{1/2}$ (dog) = 18 hr

29b-S
SC-75416

AirPouch ED_{50}[a]	Edema ED_{50}[b]	Hyperalgesia ED_{50}[c]	Arthritis ED_{50}[d]	hCOX-2 IC_{50}[e]
0.43 mg/kg	2.7 mg/kg	4 mg/kg	0.08 mg/kg	0.0625 μM

[a] See Ref. 2c Section 2.9.
[b,c] See Ref. 2c Section 2.10.
[d] See Ref. 2c Section 2.11.
[e] See Ref. 2c Section 2.4 and note 3.

However, to accommodate the bulky 7-*t*-butyl substituent, the entire membrane binding helix cluster moved ~0.7 Å away from the active site, and the side chain of Tyr355 moved 1.6 Å. The detailed interaction of the COX enzymes with the membrane are not known, but it is interesting that such a large concerted motion is required for binding of this compound and that its in vitro and in vivo potency appear unimpaired.

Based on these data in Table 4, we evaluated the 6-Cl-7-subitituted analogs in an in vitro human liver microsomal assay. Compounds containing alkyl, alkoxy, and alkyl-amino moieties showed greater than 15% phase-1 oxidative or reductive metabolism in vitro. A group of compounds displaying good in vivo potency in the rat air pouch model (>50% inhibition of PGE_2) were resolved by chiral chromatography (Table 5).

The benzopyran series described here represents two distinct chemical series with respect to the COX-2 binding mode, preferred chirality, and resulting SAR pattern. Potent and selective COX-2 inhibitors can be made from both the *S*- and *R*-isomers, depending on the length of the 7-substituent. When the analogs contain short (up to two non-hydrogen atoms) groups at the 7-position, the *S*-isomer **29b**-(***S***) dominates. Analogs (**29c–e** and **32a–b**) with a longer chain at the 7-position (three or more non-hydrogen atoms) bind preferentially as the *R*-isomer. Retention of affinity and selectivity while completely altering the binding mode and chirality is both novel and unexpected. Compounds **29b**-(***S***) (SC-75416) displayed excellent in vitro potency, selectivity and efficacy in the air pouch (100% inhibition at 2 mpk). The PK profile of **29b**-(***S***) met all of our design criteria and **29b**-(***S***) was advanced to further in vivo studies. Both acute and chronic in vivo studies demonstrated that **29b**-(***S***) was superior to NSAIDs and other COX-2 selective inhibitors (Table 6).[2c]

In summary, we have discovered a new series of potent, orally bioavailable, selective COX-2 inhibitors structurally very distinct from the diaryl heterocycle class. In vivo they are among the most potent and anti-inflammatory and analgesic COX-2 inhibitors yet described. Additionally, compounds from these series possess high water solubility as their corresponding carboxylate salts providing the possibility of alternative formulation and dosing strategies. We successfully applied a filter requiring phase-1 metabolism as a cornerstone in our selection criteria, which resulted in the discovery **29b**-(***S***) (SC-75416). **29b**-(***S***) exhibited a human half-life of 34 h, appropriate for once-a-day dosing and demonstrated very analgesic efficacy in a clinical phase II trial of post surgical dental pain.[2c] In part 2 of this series, we described application of phase-1 metabolism as a cornerstone in our selection criteria. Part 3 of this series will detail our strategy for compound selection using a microdosing clinical protocol.

Acknowledgments

The authors thank J. Gierse, C. M. Kobldt, Y. Zhang, B. S. Zweifel for providing in vitro and in vivo data, J. Collins, P. Kleine, A. Libby, K. Palmquist for scale up and chiral purification, M. Baratta, R. Ridgewell, A. Breau for in vitro metabolism and PK study, J. L. Pierce for protein expression, J. K. Gierse for protein purification, T. A. Stults and H. E. Narepekha for crystallization, and W. C. Stallings for helpful discussions.

Supplementary data

Supplementary data associated with this article can be found, in the online version, at doi:10.1016/j.bmcl.2010.07.054.

References and notes

1. (a) Wang, J. L.; Carter, J.; Kiefer, J. R.; Kurumbail, R. G.; Pawlitz, J. L.; Brown, D.; Hartmann, S. J.; Graneto, M. J.; Seibert, K. S.; Talley, J. J. *Bioorg. Med. Chem. Lett.*, submitted for publication; (b) The Pfizer Institutional Animal Care and Use Committee reviewed and approved the animal use in these studies. The animal care and use program is fully accredited by the Association for Assessment and Accreditation of Laboratory Animal Care, International.
2. (a) Zhang, Y.; Shaffer, A.; Portanova, J.; Seibert, K.; Isakson, P. C. *J. Pharmacol. Exp. Ther.* **1997**, *283*, 1069–1075; (b) Portanova, J. P.; Zhang, Y.; Anderson, G. D.; Hauser, S. D.; Masferrer, J. L.; Seibert, K.; Gregory, S. A.; Isakson, P. C. *J. Exp. Med.* **1996**, *184*, 883–891; (c) Gierse, J.; Nickols, M.; Leahy, K.; Warner, J.; Zhang, Y.; Cortes-Burgos, L.; Carter, J.; Seibert, K.; Masferrer, J. *Eur. J. Pharmacol.* **2008**, *588*, 93.
3. The modified enzyme assays (Ref. 4) was created to identify inhibitors that exhibit slow 'off-rate' kinetics due to tight binding to their target enzyme, the traditional enzyme assay (Ref. 2c) may not be optimal for characterization of compounds from alternative classes that exhibit different kinetics for inhibition. Further, such assays may provide substantially different IC_{50} values with subtle changes in assay protocol.
4. Aston, K. W.; Brown, D. L.; Carter, J. S.; Deprow, A. M.; Fletcher, T. R.; Hallinan, E. A.; Hamper, B. C.; Huff, R. M.; Kiefer, J. R., Jr.; Koszyk, F.; Kramer, S. W.; Liao, S.; Limburg, D.; Springer, J. R.; Tsymbalov, S.; Wang, L. J.; Xing, L.; Yu, Y. WO 04087687 A1, 2004.
5. X-ray structure coordinates for all complexes have been deposited into the Protein Data Bank with accession codes 3NTG (**23d**-(***R***)) and 3MQE (**29b-**(***S***)). Data for the crystal structures described herein were collected at IMCA-CAT (17-ID) beamline at the Advanced Photon Source and was supported by the companies of the Industrial Macromolecular Crystallography Association through a contract with the Center for Advanced Radiation Sources at the University of Chicago.
6. (a) Picot, D.; Loll, P. J.; Garavito, R. M. *Nature* **1994**, *367*, 243; (b) Kurumbail, R. G.; Stevens, A. M.; Gierse, J. K.; McDonald, J. J.; Stegeman, R. A.; Pak, J. Y.; Gildehaus, D.; Miyashiro, J. M.; Penning, T. D.; Seibert, K.; Isakson, P. C.; Stallings, W. C. *Nature* **1996**, *384*, 644.